文章编号：1001-9014(2021)06-0749-05

DOI：10.11972/j.issn.1001-9014.2021.06.007

0.825 THz GaAs monolithic integrated sub-harmonic mixer

LIU Si-Yu[1,2], ZHANG De-Hai[1*], MENG Jin[1], JI Guang-Yu[2], ZHU Hao-Tian[1], HOU Xiao-Xiang[3], ZHANG Qing-Feng[3]

(1. Key Laboratory of Microwave Remote Sensing, National Space Science Center, Chinese Academy of Sciences, Beijing 100190, China;
2. University of Chinese Academy of Sciences, Beijing 100049, China;
3. Southern University of Science and Technology, Shenzhen 518055, China)

Abstract: A sub-harmonic monolithic mixer with a center frequency of 0.825 THz is developed based on GaAs monolithic microwave integrated circuit technology. The parasitic parameters of the anti-parallel Schottky diode at the terahertz frequency are analyzed to improve the circuit design. The monolithic circuit is suitable for terahertz devices with the characteristics of high integration and little fabrication deviation. Meanwhile, the beamlead circuit is used to reduce the loss of substrate and installation position offset. Measured results show that the single-sideband (SSB) conversion loss of the mixer is lower than 33 dB in the frequency range 0.81~0.84 THz, and the minimum SSB conversion loss is 28 dB.

Key words: anti-parallel Schottky diode, conversion loss, monolithic microwave integrated circuit, terahertz mixer

PACS: 07.57.Kp, 84.30.r, 84.30.Qi, 84.30.Vn, 85.30.De

0.825 THz砷化镓单片集成二次谐波混频器

刘锶钰[1,2], 张德海[1*], 孟 进[1], 纪广玉[2], 朱皓天[1], 侯晓翔[3], 张青峰[3]

(1. 中国科学院国家空间科学中心 微波遥感技术重点实验室,北京 100190;
2. 中国科学院大学,北京 100049;
3. 南方科技大学,广东 深圳,518055)

摘要:基于国内的GaAs单片集成电路产线,研制了一款中心频率在0.825 THz的二次谐波单片混频器。针对肖特基二极管在太赫兹频段的高频效应详细分析了反向并联肖特基二极管的寄生参数以完善单片电路的设计。单片电路集成度高和装配误差小的特性更适用于太赫兹频段器件的设计。梁氏引线形式电路设计既可以降低介质基板带来的损耗,减小安装的位置偏移。实测结果表明,0.825 THz单片混频器最佳单边带的插损值为28 dB,0.81到0.84 THz频率范围内插损小于33 dB。

关 键 词:反向并联肖特基二极管;插入损耗;集成单片电路;太赫兹混频器

中图分类号:TN454;TN773.2 **文献标识码**:A

Introduction

The terahertz wave is between microwave and optical wave, which has huge applications[1]. Terahertz waves have a low quantum energy, good security, and wide frequency band, which is worthy of academic research and applications[2-4]. These waves have wide application prospects in the fields of security imaging, terahertz communication, and terahertz spectrum analysis[5-6]. Research on devices and systems at high terahertz frequencies is sparse due to the limitation of monolithic microwave integrated circuit technology and the lack of terahertz sources. The development of terahertz devices provides the technical basis for detecting ice-

Received date: 2021-03-09, **revised date**: 2021-04-16 **收稿日期**:2021-03-09,**修回日期**:2021-04-16

Foundation tiem: Youth Innovation Promotion Association CAS (E1213A04)

Biography: LIU Si-Yu(1994-), female, Liaoning China, doctoral candidate. Research area involves solide-state terahertz circuit and terahertz application. E-mail: liusiyu1217@126.com

***Corresponding author**: E-mail: zhangdehai@mirslab.cn

cloud information, which can be further improved through detection above 0.8 THz, at which meteorological changes can be more accurately forecast and some natural disasters prevented in advance[7]. With increasingly deeper exploration of terahertz applied fields, terahertz devices are being developed with higher frequency and better performance[8-14]. Thomas designed an 835~900 GHz fundamental balanced mixer with 9.25 dB conversion loss[15]. And Thomas, *et al.* designed an 874 GHz sub-harmonic balanced mixer. The optimal conversion loss of this mixer is 10 dB and the 3 dB bandwidth ranges from 820 to 920 GHz[16]. Zhang Bo, *et al.* designed a 1.1 THz tenth-harmonic mixer based on a planar GaAs Schottky diode. Measurement results show that the conversion loss is less than 55 dB in the frequency range 1.03~1.154 THz[17].

The design of a sub-harmonic mixer above 0.8 THz and the associated processing measurements have been completed in the present work. The core component of the proposed terahertz mixer is an anti-parallel Schottky diode, which shows a complex high frequency parasitic effect in the terahertz range. The analysis and modeling of Schottky diodes is the key to the design of a monolithic circuit, which will bring more advantages to realize matching circuit and to achieve better performance of mixer[18-19]. Further study on the high frequency parasitic parameter model of a Schottky diode is of great value for the design of a 0.825 THz monolithic mixer circuit.

1 Schottky diode modeling

A Schottky diode is an important component of conversion devices in terahertz. It is necessary to analyze the diode model deeply for a better circuit match to improve device performance. The structure of a Schottky diode consists of a high electron mobility substrate, low doping buffer layer, high doping epitaxial layer, and upper metal structure, as shown in Fig. 1.

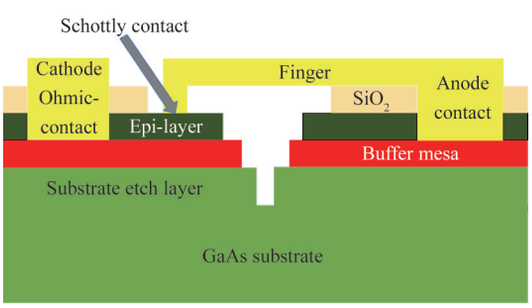

Fig. 1 Three-dimensional cross-sectional view of Schottky diode
图1 肖特基二极管的三维横截面图

A Schottky diode is mainly composed of intrinsic parameters and high frequency parasitic parameters. The intrinsic parameters reflect the DC characteristics of Schottky diodes, including ideal factor n, saturation current I_{sat}, zero-bias junction capacitance C_{j0}, and series resistance R_s[20]. These characteristics determine the cutoff frequency of the diode and play an important role in the matching of the entire circuit.

$$I_{sat} = RC \cdot A_a T^2 \left(e^{-\frac{q\Phi}{kT}}\right) \quad , \quad (1)$$

$$I(V) = I_{sat} \cdot \left(e^{\frac{qV}{nkT}} - 1\right) \quad , \quad (2)$$

$$C_{j0} = \left(C_t - C_{pp}\right)/N - C_{fp} \quad , \quad (3)$$

$$C_j(V_j) = A\sqrt{\frac{q\varepsilon_s N_d}{2(V_{bi} - V_j)}} = \frac{C_{j0}}{\sqrt{1 - (V_j/V_{bi})}} \quad , \quad (4)$$

$$R_s(V_j f) = R_{epi}(V_j f) + R_{spreading}(f) + R_{ohmic}(f). \quad (5)$$

In this design, the Schottky diode anode diameter is 0.8 μm and epitaxial layer thickness 0.1 μm. According to the above formula, $I_{sat} = 3 \times 10^{-17} A$, $C_{j0} = 1fF$, and $R_s = 15\ \Omega$.

However, the high frequency parasitic parameters of the diode cannot be ignored because of the great influence on the design of devices in terahertz. The high frequency effect of a Schottky diode is seldom studied due to the vacancy of on-chip test probe platforms. A detailed theoretical analysis and simulation verification of high-frequency parasitic parameter extraction are carried out by the parameter matrix, which mainly includes the parasitic capacitance C_{pp} between anode and cathode pads, parasitic inductance L_f and parasitic resistance R_f of the air bridge finger, and parasitic capacitance C_{fp} between air bridge and pad[21-24]. The top view of the anti-parallel Schottky diode is shown in Fig. 2.

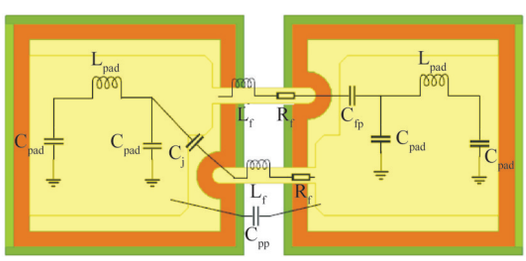

Fig. 2 Top view of anti-parallel Schottky diode
图2 反并联肖特基二极管俯视图

The anode and cathode pad structure can be equivalent to the π-type circuit composed of capacitance C_{pad} and inductance L_{pad}, the finger can be equivalent to the series circuit of finger inductance L_f and finger resistance R_f, and the anode column part can be equivalent to the parallel circuit of parasitic capacitance C_{fp} between finger and pad parallel capacitance C_j and resistance R_j of the Schottky-junction contact. The equivalent circuit of an anti-parallel Schottky diode for four-step parameter extraction is shown in Fig. 3, where ① is the equivalent circuit of the pad, ② is the equivalent circuit between the anode and cathode pad, ③ is the equivalent circuit of the finger, and ④ is the equivalent circuit between the finger and pad.

The Y parameters of the anode or cathode pad structure $\boldsymbol{Y}_{pad}$, no finger structure $\boldsymbol{Y}_{pad-pad}$, finger connected structure $\boldsymbol{Y}_{finger(n)}$, and finger pad part $\boldsymbol{Y}_{pad-finger}$, are calculated as follows, where n is the number of fingers, n = 1, 2.

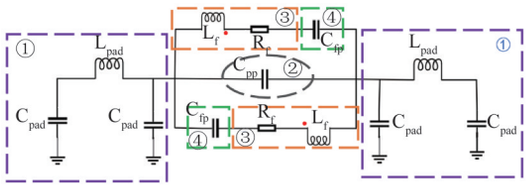

Fig. 3　Equivalent circuit of anti-parallel Schottky diode
图3　反向并联肖特基二极管等效电路

$$\boldsymbol{Y}_{pad}=\begin{bmatrix}\dfrac{1}{j\omega C_{pad}}+j\omega L_{pad} & -j\omega L_{pad}\\ -j\omega L_{pad} & \dfrac{1}{j\omega C_{pad}}+j\omega L_{pad}\end{bmatrix}$$

$$\boldsymbol{Y}_{pad-pad}=\begin{bmatrix}j\omega C_{pp} & -j\omega C_{pp}\\ -j\omega C_{pp} & j\omega C_{pp}\end{bmatrix}$$

$$\boldsymbol{Y}_{finger(n)}=\begin{bmatrix}\dfrac{1}{j\omega L_{f(n)}+R_{f(n)}} & -\dfrac{1}{j\omega L_{f(n)}+R_{f(n)}}\\ -\dfrac{1}{j\omega L_{f(n)}+R_{f(n)}} & \dfrac{1}{j\omega L_{f(n)}+R_{f(n)}}\end{bmatrix}$$

$$\boldsymbol{Y}_{pad-finger}=\begin{bmatrix}j\omega C_{fp} & -j\omega C_{fp}\\ -j\omega C_{fp} & j\omega C_{fp}\end{bmatrix} \quad . \quad (6)$$

The Y parameters of each part can be calculated from the simulation, where $\boldsymbol{Y}_{T-pp}$ is the no finger structure parameter; $\boldsymbol{Y}_{T-f(n)}$ the finger short structure parameter, where $n=1$ or 2 and $\boldsymbol{Y}_{T-fp}$ the no Schottky-junction structure parameter.

$$\boldsymbol{Y}_{pad-pad}=\boldsymbol{Y}_{T-pp},\ \boldsymbol{Y}_{finger(n)}=\boldsymbol{Y}_{T-f(n)}-\boldsymbol{Y}_{T-pp}$$

$$\boldsymbol{Y}_{pad-finger}=\frac{1}{\boldsymbol{Y}_{T-fp}-\boldsymbol{Y}_{T-pp}}-\frac{1}{\boldsymbol{Y}_{T-f(2)}-\boldsymbol{Y}_{T-pp}}. \quad (7)$$

From the above simulated Y-parameters, the component values of the parasitic equivalent circuit are the following:

$$C_{pad}=\frac{1}{\omega \boldsymbol{Y}_{pad11}+\omega \boldsymbol{Y}_{pad12}} \quad L_{pad}=\frac{-\boldsymbol{Y}_{pad12}}{\omega} \quad , \quad (8)$$

$$C_{pp}=\frac{\boldsymbol{Y}_{T-pp11}}{\omega} \quad , \quad (9)$$

$$L_{f(n)}=\frac{1}{\omega(\boldsymbol{Y}_{T-f(n)}-\boldsymbol{Y}_{T-pp})_{11}} \quad , \quad (10)$$

$$R_{f(n)}=re\left\{\frac{1}{(\boldsymbol{Y}_{T-f(n)}-\boldsymbol{Y}_{T-pp})_{11}}\right\} \quad , \quad (11)$$

$$C_{fp}=\left\{\frac{1}{\boldsymbol{Y}_{T-fp}-\boldsymbol{Y}_{T-pp}}-\frac{1}{\boldsymbol{Y}_{T-f(2)}-\boldsymbol{Y}_{T-pp}}\right\}_{11}/\omega \quad . (12)$$

According to the above formula and the simulated S parameters of the Schottky diode, the high frequency parasitic parameters can be calculated as follows: $C_{pp}=4.5\,fF$, where C_{pp} varies with the distance between the anode and cathode pad. $R_{f(1)}=0.5\,\Omega$, $L_{f(1)}=55$ pH, and $L_{f(2)}=70$ pH, which are related to finger width and distance between fingers.

$$M=\left(L_{f(1)}+L_{f(1)}-L_{f(2)}\right)/2 \quad , \quad (13)$$

M is the mutual inductance between two fingers, which is a special parasitic parameter of an anti-parallel Schottky diode. The anode pad, cathode pad, and fingers play an important role in the formation of high frequency parasitic parameters. A more reasonable design of a Schottky diode model can reduce high-frequency parasitic parameters to achieve a better design.

2　Mixer design

A beamlead monolithic circuit is used to realize the installation of the circuit and cavity in the design of the 0.825 THz sub-harmonic mixer, which not only reduces the loss caused by the dielectric substrate, but also reduces the installation position offset. The design of the sub-harmonic mixer mainly includes radio frequency (RF) and local oscillator (LO) probes, LO and intermediate frequency (IF) low-pass filters, and the anti-parallel Schottky diode. A WR1 rectangular waveguide is used as the RF waveguide in the frequency range 0.75~1.1 THz, and a WR2.2 rectangular waveguide as the LO waveguide in the frequency range 0.33~0.5 THz. The beam lead circuit is installed in the cavity with a small amount of conductive adhesive [25]. The proposed 0.825 THz mixer architecture and assembled mixer block are shown in Fig. 4.

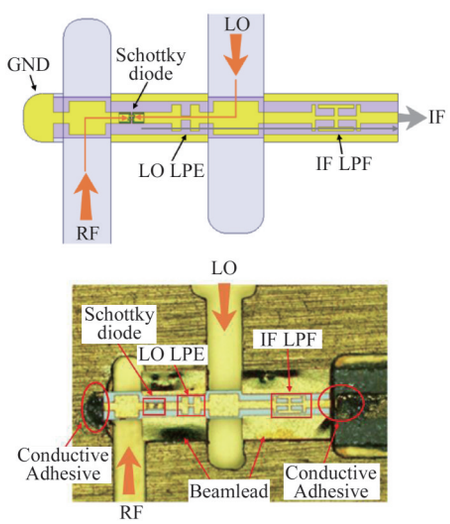

Fig. 4　Proposed 0.825 THz mixer architecture and assembled mixer block
图4　关于0.825 THz混频器模块结构及安装图

Simulated results show that the SSB conversion loss of this mixer is 9 dB in the range 0.815~0.835 THz, and the minimum SSB conversion loss is 7.8 dB. The simulated conversion loss of the 0.825 THz sub-harmonic mixer is shown in Fig. 5.

For the proposed 0.825 THz mixer design, the LO low-pass filter (LPF) adopts the form of three high and low impedance lines, which has a simple structure and wide bandwidth. The IF LPF [26] is different from the LO LPF and has compact microstrip resonating cell (CMRC) structure. The length of the LO LPF is 149 μm and the length of the CMRC for the IF LPF is 230 μm. Simulated results from the two LPFs are shown in Fig. 6.

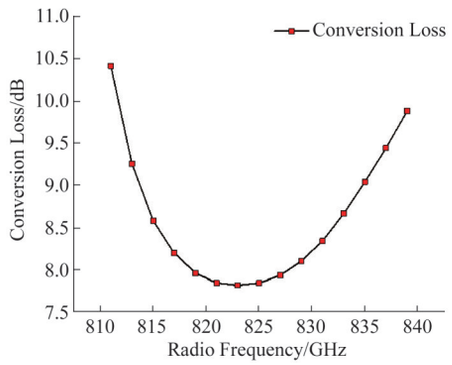

Fig. 5 Simulated 0. 825 THz sub-harmonic mixer performance
图5 关于0. 825 THz二次谐波混频器仿真结果

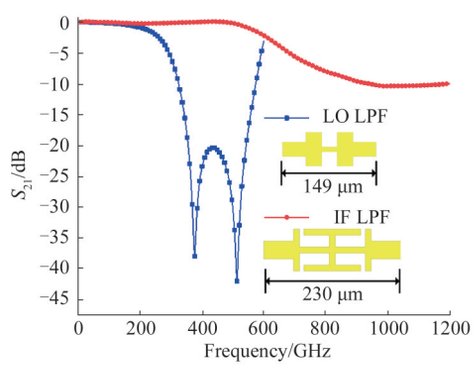

Fig. 6 Comparison of two different IF LPFs
图6 两个不同中频低通滤波器结果对比

3 Measurement and discussion

The performance of the proposed 0. 825 THz subharmonic mixer was measured by fixed IF frequency, and the construction of the subharmonic mixer test platform is depicted in Fig. 7. The RF and LO are input into the mixer, and the IF power is measured by a spectrometer.

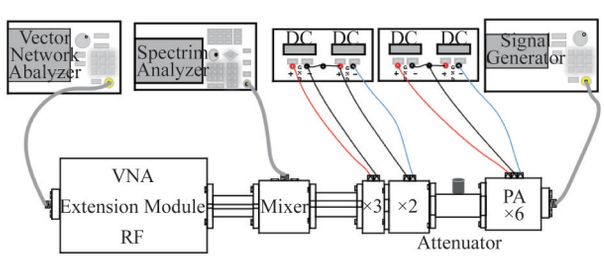

Fig. 7 Sub-harmonic mixer performance measurement platform for 0. 825 THz
图7 关于0. 825 THz二次谐波混频器测试平台

The signal generator operates at 11. 1~11. 7 GHz. To provide the 0. 4~0. 42 THz LO signal with 4 mW, the signal generator was cascaded by a sextupler, attenuator, doubler and tripler. The RF source is provided by a 0. 75~1. 1 THz extender, and the IF output is obtained by a spectrum analyzer. The measured performance of the proposed 0. 825 THz sub-harmonic mixer is shown in Fig. 8. It can be observed from the figure that the measured SSB conversion loss is 28~33 dB over the frequency range 0. 81~0. 84 THz, and the minimum SSB conversion loss is 28 dB at 0. 836 THz.

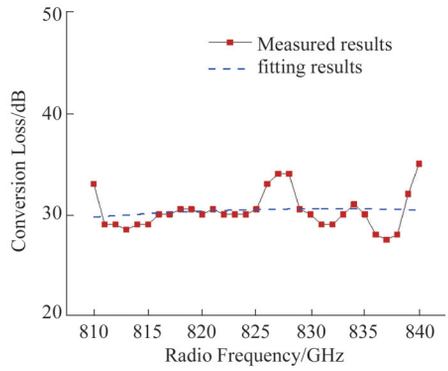

Fig. 8 Measured 0. 825 THz sub-harmonic mixer performance
图8 关于0. 825 THz二次谐波混频器测试结果

There is difference between the measured and simulated results due to the circuit size sensitivity of terahertz devices, for which a small deviation will have a great impact on the final results. Because the ratio between circuit size and wavelength cannot be ignored, the processes of monolithic circuit processing, cavity processing, and installation have great influence. During measurement, the loss of the RF source is caused by the gap between the flange of the extender and that of the RF waveguide, the position deviation of the waveguide port, and the roughness of waveguide. There is approximately a 5 dB loss when the gap between the two flanges is 30 μm, and approximately a 3 dB loss when the position deviation of the waveguide port is 40 μm in simulation. It is easy to produce position deviation in the connection of measurement equipment, which cannot be ignored at terahertz frequencies. More attention will be paid to the avoidance of assembly deviation in the next planned design. The deviation between the simulated and measured results may be due to the inaccurate simulation model, processing error, assembly error and measurement error. Although many uncontrollable deviations have an influence on the performance of the proposed 0. 825 THz mixer, its design is preliminarily realized.

4 Conclusions

A monolithic mixer is designed in the form of a beamlead circuit based on a 15 μm thick GaAs substrate. A more reasonable anti-parallel Schottky diode model is designed based on the analysis of the intrinsic parameters and high-frequency parasitic effect of the Schottky diode. Measured results show that the SSB conversion loss of the proposed 0. 825 THz mixer is lower than 33 dB in the range 0. 81~0. 84 THz, and the minimum SSB conversion loss is 28 dB at 0. 836 THz. The deviation that may be introduced in the measurement of a terahertz monolithic mixer can influence the conversion loss of the mixer. The measured results of the 0. 825 THz monolithic mixer prove that monolithic circuit design will become one of the important directions of future terahertz

device design. More in-depth analysis of the diode model, greater tolerance in circuit design, and smaller deviation in the assembly measurement process are several problems that will be solved in the monolithic design.

References

[1] Siegel P H. Terahertz technology [J]. *IEEE Transactions on Microwave Theory and Techniques*, 2002, **50**(3): 910-928.

[2] Jasteh D, Hoare E G, Cherniakov M, *et al*. Experimental low-terahertz radar image analysis for automotive terrain sensing [J]. *IEEE Geoscience and Remote Sensing Letters*, 2016, **13**(4):490-494.

[3] Siegel P H. Terahertz technology in biology and medicine [C]. USA, IEEE MTT-S International Microwave Symposium Digest, 2004: 1575-1578.

[4] Siegel P H. THz instruments for space[J]. *IEEE Transactions on Antennas and Propagation*, 2007, **55**(11):2957-2965.

[5] Chen Z, Ma X Y, Zhang B, *et al*. A survey on terahertz communications[J]. *China Communications*, 2019, **16**(2):1-35.

[6] Song H, Nagatsuma T. Present and future of terahertz communications[J]. *IEEE Transactions on Terahertz Science and Technology*, 2011, **1**(1):256-263.

[7] Zhang Z, Monosmith B. Dual-643 GHz and 874 GHz airborne radiometers for ice cloud measurements[C]. USA, IGARSS IEEE International Geoscience and Remote Sensing Symposium, 2008.

[8] Maagt de P. Terahertz technology for space and EARTH applications [C]. UK, International workshop on Antenna Technology, 2007: 111-115.

[9] LIU Ge, ZHANG Bo, ZHANG Li-Sen, *et al*. 0.42 THz subharmonic mixer based on 3D precisely modeled diode [J]. *Journal of infrared and millimeter waves*, (刘戈,张波,张立森,等。基于二极管3D精确模型的0.42 THz分谐波混频器。**红外与毫米波学报**)2018, **37**(3):338-343.

[10] Albrecht J D, Rosker M J, Wallace H B, *et al*. THz electronics projects at DARPA: Transistors, TMICs, and amplifiers [C]. USA, IEEE MTT-S International Microwave Symposium, 2010.

[11] JIANG Jun, HE Yue, WANG Cheng, *et al*. 0.67 THz sub-harmonic mixer based on Schottky diode and hammer-head filter [J]. *Journal of Infrared Millimeter Waves*, (蒋均,何月,王成,等。基于Schottky二极管和Hammer-Head滤波器0.67 THz二次谐波混频器。**红外与毫米波学报**)2016, **35**(4):418-424.

[12] JI Guang-Yu, ZHANG De-Hai, Meng Jin, *et al*. Design of a 670 GHz fourth-harmonic mixer based on Schottky diode [J]. *Journal of Infrared Millimeter Waves*, (纪广玉,张德海,孟进,等。基于肖特基二极管的四次谐波混频器。**红外与毫米波学报**)2019, **38**(6): 695-700

[13] MAO Yan-Fei, E Shi-Ju, SCHMALZKlaus ,*et al*. A low power 245 GHz subharmonic receiver [J]. *Journal of Infrared Millimeter Waves*, (毛燕飞,鄂世举,SCHMALZKlaus,等。一种低功耗245 GHz次谐波接收机。**红外与毫米波学报**)2019, **38**(6):739-744.

[14] LIU Ge, ZHANG Bo, ZHANG Li-Sen, *et al*. 330 GHz GaAs monolithic integrated sub-harmonic mixer[J]. *Journal of infrared and millimeter waves*,(刘戈,张波,张立森,等。330 GHz砷化镓单片集成分谐波混频器。**红外与毫米波学报**)2017, **36**(02):252-256.

[15] Thomas B, Maestrini A, Gill J, *et al*. A broadband 835~900 GHz fundamental balanced mixer based on monolithic GaAs membrane Schottky diodes [J]. *IEEE Transactions on Microwave Theory and Techniques*, 2010, **58**(7):1917-1924.

[16] Thomas B, Maestrini A, Matheson D, *et al*. Design of an 874 GHz biasable sub-harmonic mixer based on MMIC membrane planar schottky diodes [C]. USA, 33rd International Conference on Infrared, Millimeter and Terahertz Waves, 2008.

[17] ZHANG Bo, LV Xiao-Lin, HE Jie, *et al*. 1.1 THz tenth harmonic mixer based on planar GaAs Schottky diode[J]. *IET Microwaves, Antennas & Propagation*, 2019, **13**(11).

[18] Zhang Y, Zhao W, Wang Y F, *et al*. A 220 GHz subharmonic mixer based on Schottky diodes with an accurate terahertz diode model [J]. *Microwave and Optical Technology Letters*, 2016, **58**(10): 2311-2316.

[19] Schlecht E, Siles V J, Lee C, *et al*. Schottky diode based 1.2 THz receivers operating at room-temperature and below for planetary atmospheric sounding [J]. *IEEE Transactions on Terahertz Science and Technology*, 2014, **4**(6):661-669.

[20] Tang A Y, Stake J. Impact of eddy currents and crowding effects on high-frequency losses in planar Schottky diodes [J]. *IEEE Transactions on Electron Devices*, 2011, **58**(10):3260-3269.

[21] Ren T H, Zhang Y, Liu S, *et al*. A Study of the parasitic properties of the Schottky barrier diode [J]. *Journal of Infrared Millimeter and Terahertz Waves*, *2017*, 38:143-154.

[22] Tang A Y, Drakinskiy V, Yhland K, *et al*. Analytical extraction of a Schottky diode model from broadband S-Parameters [J]. *IEEE Transactions on Microwave Theory and Techniques*, 2013, **61**(5): 1870-1878.

[23] Tang A Y, Bryllert T, Stake J. Geometry optimization of THz subharmonic Schottky mixer diodes [C]. Australia, 37th International Conference on Infrared, Millimeter, and Terahertz Waves, 2012.

[24] Qi L W, Liu X Y, Meng J, *et al*. Improvements in reverse breakdown characteristics of THz GaAs Schottky barrier varactor based on metal-brim structure [J]. *Chinese Physics B*, 2020, **29**(5): 057306-5.

[25] Ding J Q, Maestrini A, Gatilova L, *et al*. A 300 GHz power-combined frequency doubler based on E-plane 90°-hybrid and Y-junction[J]. *Microwave Optical Technology Letters*, 2020, **62**(8): 2683-2691.

[26] Xue Q, Kam M S, Chi H C. Low conversion-loss fourth subharmonic mixers incorporating CMRC for millimeter-wave applications [J]. *IEEE Transactions on Microwave Theory and Techniques*, 2003, **51**(5):1449-1454.